ANALYSIS OF STRUCTURE, CINEMATIC AND USE MATERIALS OF FAIRHILD MECHANISM

Alimnazarov Olim Mengliboyevich

Assistant of Termez branch of Tashkent State Technical University

Dustmurodov Jahongir Mirzoalievich

Assistant of Termez branch of Tashkent State Technical University

Saynazov Jasur Holmirzaevich

Assistant of Termez branch of Tashkent State Technical University

Shamayev Yigitali Jummaevich

Assistant of Termez branch of Tashkent State Technical University

http://dx.doi.org/10.26739/2433-202x

Issue DOI http://dx.doi.org/10.26739/2433-202x-209-2020-1-6

Article DOI http://dx.doi.org/10.26739/2433-202x-2020-1-6-17

Abstract: The structural and kinematic analysis of the Fairchild mechanism is examined, and its kinematic features are presented in analytical form. The mechanism includes concepts describing theoretical and actual profiles of clustered domains.

Keywords: piston mechanism, Fairchild mechanism, cam profile, kinematic analysis.

Introduction

Improvement of piston machines remains relevant from the moment of their commissioning. In this case, the main attention of specialists is focused on improving their technological, economic and operational indicators. Important parts of research conducted in this direction are based on improving the technology and production characteristics, optimizing their geometric shapes and work processes, improving the components of crank mechanisms.

As a result of the widespread use of the entire design of the implemented mechanism, the conclusions drawn from it: reliability, compactness and other characteristics, the crank mechanism is considered more convenient than the previous one, but it is not without drawbacks. [1]

Therefore, research is currently underway aimed at the production and improvement of existing crank mechanisms of machines with energy-efficient, economical performance and a high level of reliability.

Obviously, these studies are considered to be of economic importance.

Analysis of the article

Among the many existing mechanisms providing mutual rotational motion, one can distinguish S.S. Balandin [2] and V.K. Frolov [3], their structural structure in Figure 1. These mechanisms have a number of distinctive features from others, while they are the most effective representatives of two different ways of solving the problem.

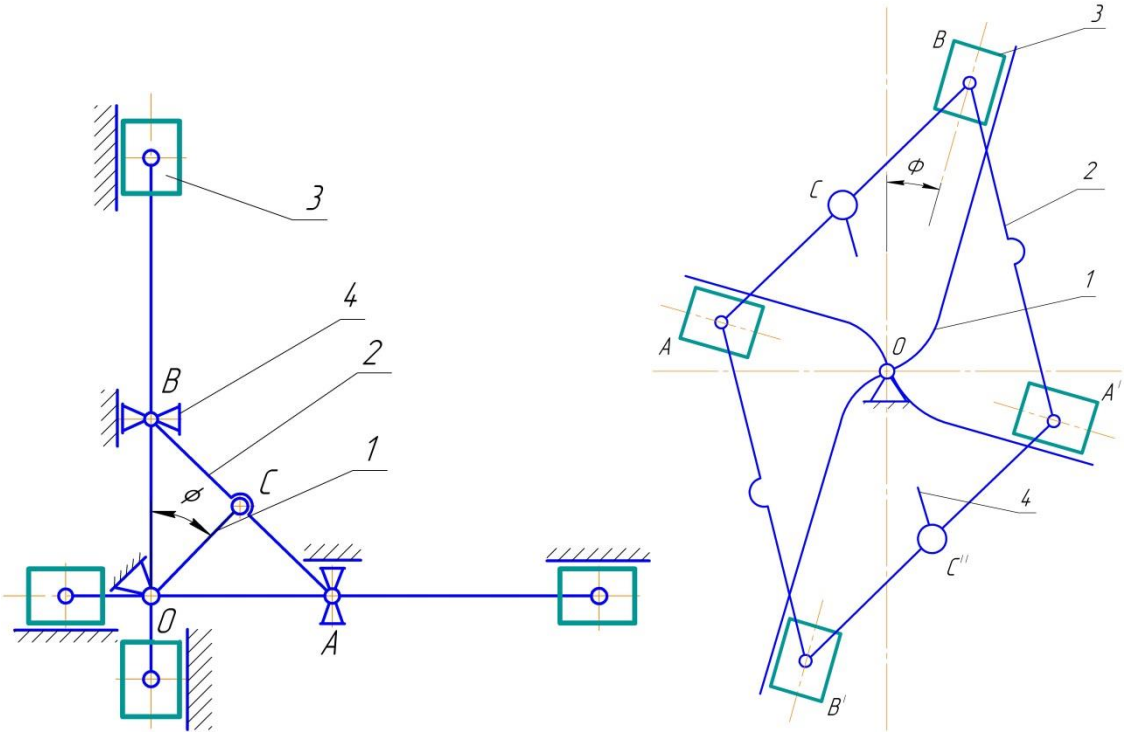

a) b)

Figure 1. Structure of mechanism
S.S. Balandin [2] and V.K. Frolov [3]

Purpose and function of the problem

The purpose of this article is to describe the kinematic analysis of the Fairchild mechanism, which combines the advantages of manual and cam mechanisms, but retained some drawbacks and a wide range of pistons. The publication of this question is practically non-existent in literature.

Design of cam profile and structure analysis of its mechanism material

The structure of the Fairchild mechanism is shown in Figure 2.

If there are introductory connections with 5 sliders (Fig. 2), then the mechanism works as follows. With a one-way operation, the gas distribution mechanism ensures the delivery of the working mixture to the gaps opposite the rotation of the output indicator of the reciprocating machine (Fig. 2 a pair of cylindrical sliders B and B). Under the action of pressure P_{im}, the pair of the selected cylindrical granules begins to move in the direction of the axis of rotation of the main shaft, which moves in the real profile of the 1st shaft and 4th roller, which leads to its rotation. The movement of the pairs of cylindrical slider B and B leads to the movement through the rods 2 (A and A) from the center of the second pair, squeezing the sacrificial working mixture from the working chambers under Pout pressure. This combination of movements leads to the “assembly" of the closed four-link $ABA'B'$. After the cam is rotated at an angle of 900, the working mixture is transferred to the second *(A and A′)* two-cylinder plane, and the process is repeated, which ensures work processes in the piston machine. Given that the movement in the

Fairchild mechanism is carried out by the movement of the rollers along the contour line of the cam, in this experiment we took into account the advisability of using materials that are resistant to food. This ensures uniform rotation of the roller along the contour without sliding during rotational and progressive movement, due to which uninterrupted rotation of the ear is achieved. To do this, steel was used, heated on a roller material to austenite area. It was heated to a temperature higher than the critical point of Ac_3, and then operated under pressure after being held for a period of time or cooling to a lower temperature than recrystallization and then at low temperatures after smearing and stripping. In this process, the conversion of a steel structure to austenite at temperatures above the critical point of Ac_3 is followed by rapid cooling after pressure processing, or conversion of austenite to martensite. The GS and ES lines are stable only at temperatures above the critical points of Ac_3 and Acm [5].

When steel is cooled very slowly from low Ar_3 and Acm to low temperatures, ferrite from pre-electrolyte steels and cemented after electrode. This will increase the hardness of the steel material. This results in high edible material, which increases the rolling resistance of the roller in the circular and forward movement of the roller and increases the life of the engine without vibration.

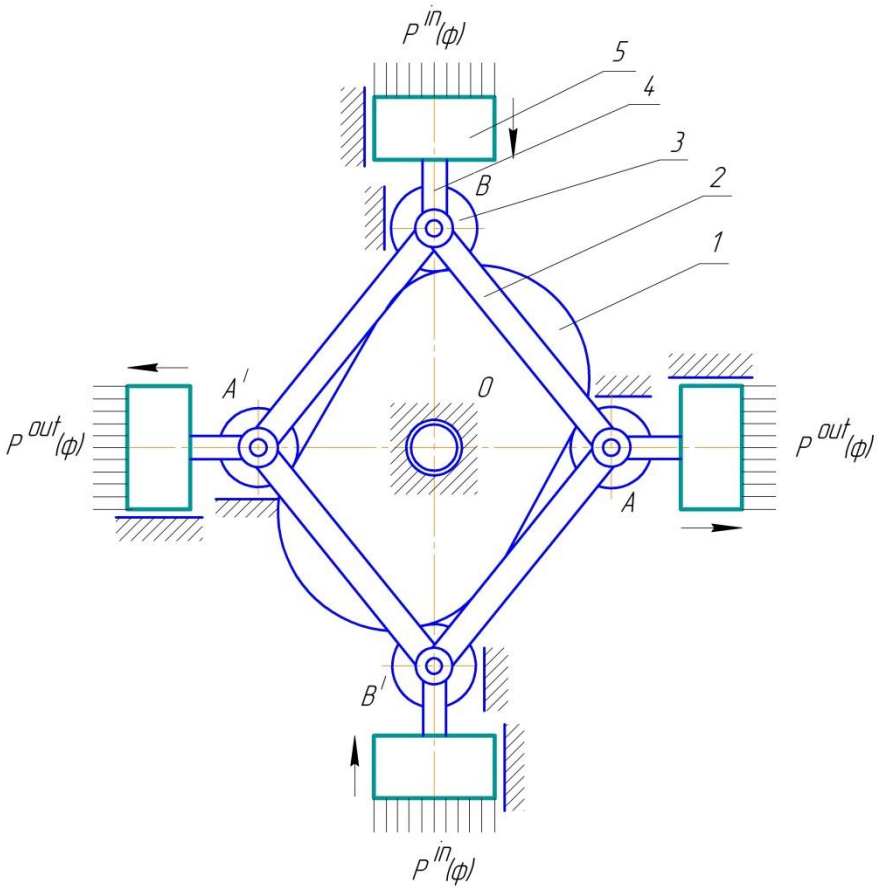

Figure 2. The structure of the Fairchild mechanism

Obviously, the number of degrees of freedom of the engine is 5 and has one main motive and four constant excessive motions, which allows the rollers to rotate freely [4].

$$w=3\cdot n-2\cdot p_{lov}-p_{high}=3\cdot 13-2\cdot 17-4=1,$$

here, n=13- the number of moving link (4 crossheads, 4 rollers, 4 rods, cams); p_{lov}=17- lower kinematic pair (13 rollers and 4 advanced); P_{high}=4- the number of higher kinematic pairs.

An explanation of these discrepancies is given in [5].

The deciding factor of this mechanism is the theoretical ear profile [4], in the case of a polar coordinate system, a-a and b-b meters (Figure 2), has the following form:

$$r(\varphi)^2 + r(90^0 - \varphi)^2 = l^2, \qquad (1)$$

here, $r(\varphi)$ – a function that describes the theoretical state of the cam; φ – the torsion angle of the cam; *l*- the length of the rod.

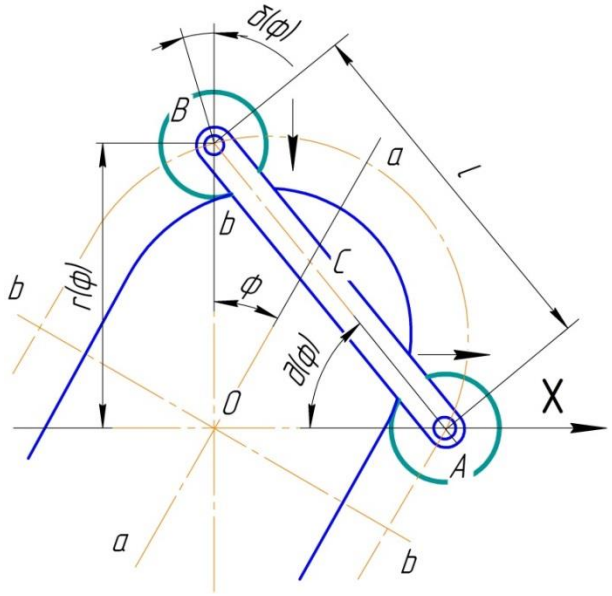

Figure 3. The following relationships are selected to determine the $r(\varphi)$ function.

$$r(0^0) - r(90^0) = S; \qquad (2)$$

$$r(0^0) = l \cdot \cos\left(\beta(0^0)\right); \qquad (3^{I})$$

Here, *S*- the step of the crosshead; $\beta(\varphi)$ – The bending angle of the link to the *Ox* axis (Figure 3).

If we take into account (1)

$$\beta(0^0) = 45^0 - arcsin\,(S/l\sqrt{2}),$$

in general

$$\beta(\varphi) = arcsin\,(r(\varphi)/l).$$

In addition to the links (3′) the conditions of the border are taken into account that the B crosshead does not change in the $\varphi = 0^0$, that is, according to the $v_B/_{\varphi=0^0} = 0$, *-dr/dφ* (for the positive direction of the B crosshead it is necessary to transfer the movement to point O), the second boundary condition for its function $r(\varphi)$

$$dr/d\varphi/_{\varphi=0^0} = 0. \qquad (3^{II})$$

performing a (3′′) will automatically fulfill the $v_A/_{\varphi=0^0} = 0$. condition.

the $r(\varphi)$ function must satisfy equation (1) and (2) and (3).

There are several ways to find a function that is specified. One of them is the representation of the square of the extended shape function of the Furye series in general $\varphi \in [0^0; 90^0]$ intervals.

$$r(\varphi)^2 = \frac{A_0}{2} + e_{k=1}A_k cos\frac{k\pi\varphi}{90^0} + B_k sin\frac{k\pi\varphi}{90^0} \qquad (4)$$

Then (1) considering equation (4)

$$A_0 + 2e_{k=1}A_{2k} cos\frac{2k\varphi}{90^0} + B_{2k-1} sin\frac{(2k-1)\pi\varphi}{90^0} = l^2$$

At the same time, the expansion coefficients A_k and B_k are found in the orthogonality features of trigonometric functions. Leaving the process, we get the final result of the structure of the solution.

$$r^2 = \frac{l^2}{2} + e_{k=1} A_{2k-1} cos \frac{(2k-1)\pi\varphi}{90^0},$$

Here, $$A_k = 480 \cdot l^2 \cdot (2cos^2(\beta(0^0)) - 1)/(\pi^6 k^6).$$

The second $r(\varphi)$ variant argument is defined by equation (1) of the $r(\varphi)$ function values for the $\varphi \in [0^0; 45^0)$, in Level 3 in the $\varphi \in [45^0; 90^0)$ range. The coefficient is calculated taking into account (2) and (3).

Obviously, the second look has the only solution (no endless series). However, it is necessary to consider 15 different sequences for the first view, and taking into account the persistence of the r argument of any $r(\varphi)$ function, it should be noted that if the expression accepted for A_k, both types of high-precision equation are also suitable.

It is necessary to compile the profile of the cam [4] and see Fig. 4, according to the parametric equation of the polar coordinate system, as follows:

$$r' = Ob;$$
$$\varphi' = \varphi - \theta,$$

here, the $Ob(\varphi)$ (rolling point of the β-cam) and the angle $\theta(\varphi)$- are calculated from the OBb triangle according to the cosine and sinus theorems.

$$Ob = \sqrt{r^2 + \rho^2 - 2r\rho\cos(\delta)}$$
$$\theta = arcsin\frac{\rho}{Ob} \cdot \sin(\delta),$$

Here, ρ- radius of the roller 3; $\delta(\varphi)$- the pressure angle, which defines the angle between the sliding velocity vector and the normal vector roller joint and the profile between cams (Fig.4, the point is denoted by b). According to the theory of mechanisms with cams [4]

$$\delta = arctg((dr/d\varphi)/r),$$

this ensure that the rotary shaft output machine is the same ($\omega = const$).

There is a limit to the maximum value of the $\delta(\varphi)$ angle, which aims to increase the efficiency of the "roller-coil" pairing and improve working conditions. The boundary value $[\delta]$ is usually between 24^0 and 30^0, so the $(\delta(\varphi)) \leq [\delta]$ maximum is the maximum when the second link *l* that defines the engine dimensions is met.

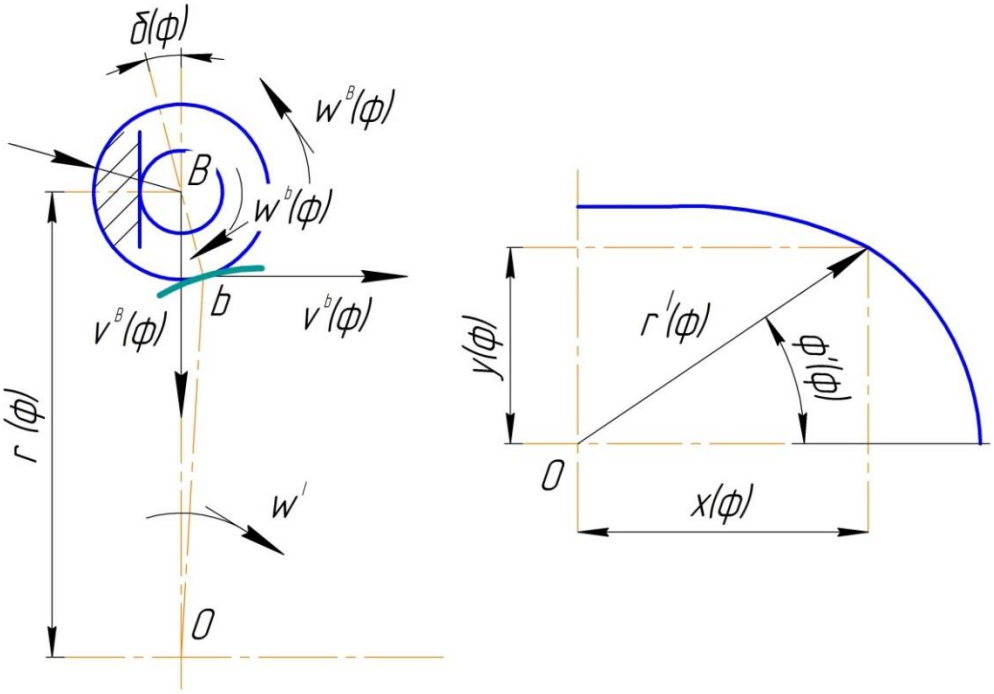

Figure 4. Determining the true ear profile in the Polar (a) and Cartesian coordinate system (b).

In the Cartesian coordinate system, it is easier to set a true profile (Fig. 5 b).

$$x = r \cdot \cos(\varphi) - \rho \cdot \cos(\varphi + \delta);$$

$$y = r \cdot \sin(\varphi) - \rho \cdot \sin(\varphi + \delta.$$

This profile identifies the curvature radius of the mechanism [6]

$$R = \left|(\dot{x}^2 + \dot{y}^2)^{3/2}/(\dot{x}\ddot{y} - \ddot{x}\dot{y})\right|.$$

Analysis of the selected material for the mechanism roller detail

The progression and rotational movement of the roller part of the mechanism along the contour line will depend on its size. The number of clips of the Fairchild mechanism will be from four to eight. The roller structure is made of carbon grade C10A or C12A grade steel, brought to 60-65 according to Rockwell, and the working surface is carefully polished, which provides high abrasion resistance during rotational and progressive movement, which increases the service life of its absorption and vibrating moving defect.

Kinematic analysis of mechanism

Determining the motion, velocity, and acceleration of point B

$$S_B = l \cdot \left(\sin\left(\beta(0^0)\right) - \sin\left(\beta(\varphi)\right)\right);$$

$$\mathrm{v}_B = \frac{dS_B}{dt} = -l \cdot \cos(\beta) \cdot \frac{d\beta}{d\varphi} \cdot \omega_1;$$

$$a_B = \frac{d\mathrm{v}_\mathrm{B}}{dt} = \frac{d\mathrm{v}_\mathrm{B}}{d\varphi} \cdot \omega_1$$

The following relationships are important for moving point, velocity, and acceleration:

$$S_A(\varphi) = S - S_B(90^0 - \varphi);$$

$$\mathrm{v}_\mathrm{A}(\varphi) = \mathrm{v}_\mathrm{A}(90^0 - \varphi);$$

$$a_A(\varphi) = -a_A(90^0 - \varphi).$$

According to the kinematics of the 2 joints given (Fig. 4), it is easier to determine the absolute velocity of their points than the angular velocity.

$$\omega_{AB} = (\mathrm{v}_\mathrm{A} \sin(\beta) + \mathrm{v}_\mathrm{B} \cos(\beta))/l,$$

It can be written according to the law of cosines as follows:

$$v_C = \sqrt{v_B^2 + \frac{(\omega_{AB} l)^2}{4} - v_B \omega_{AB} l \cdot \cos(\beta)}$$

The angular acceleration of the 2 joints is calculated based on its center of gravity.

$$\varepsilon_{AB} = (d\omega_{AB}/d\varphi) \cdot \omega_1;$$
$$a_C = (dv_C/d\varphi) \cdot \omega_1.$$

The kinematic problem of roller compound 3 is not resolved (Figure 2). If it is done as shown in Figure 5, it means 1 "push" and 2 "directional". Then it is necessary to determine the angular velocity of $\omega_B(\varphi)$ and $\omega_b(\varphi)$ respectively.

$$\omega_B = v_{B/b}/\rho;$$
$$\omega_b = v_B/\rho'.$$

Here, $v_{B/b} = v_B \sin(\delta) + v_b \cos(\theta + \delta)$ – The velocity of point B with respect to b; $v_b = \omega_1 \cdot Ob$; ρ'- roller radius of the "directional".

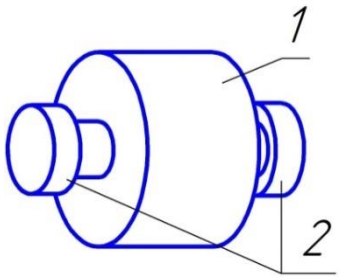

Figure 5. Roller knob

Result of kinematic analysis

The following are some of the results of the Fairchild mechanism (Figure 6). Figure 6 summarizes the analysis of the $\varphi \in [0^0; 90^0]$ intermediate nature of the change in kinematic properties of the mechanism.

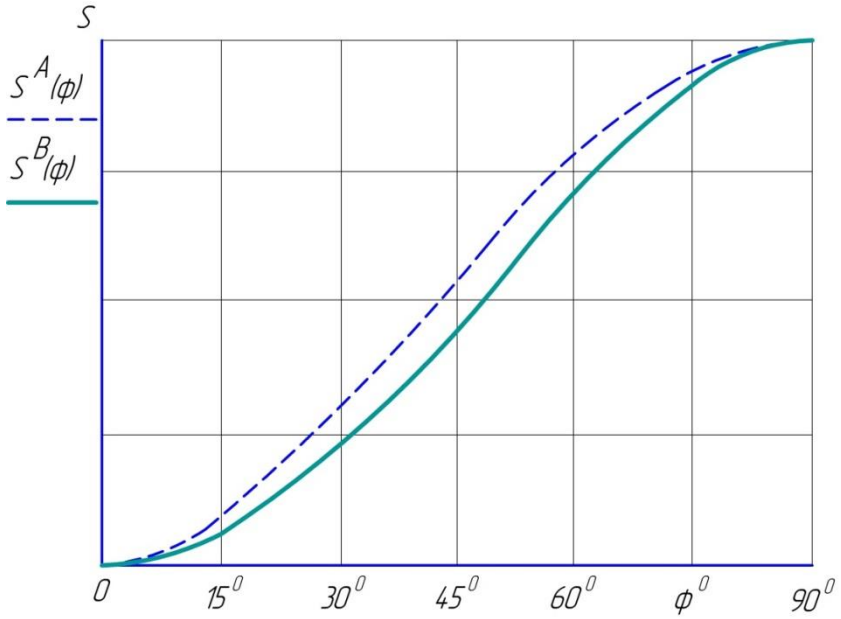

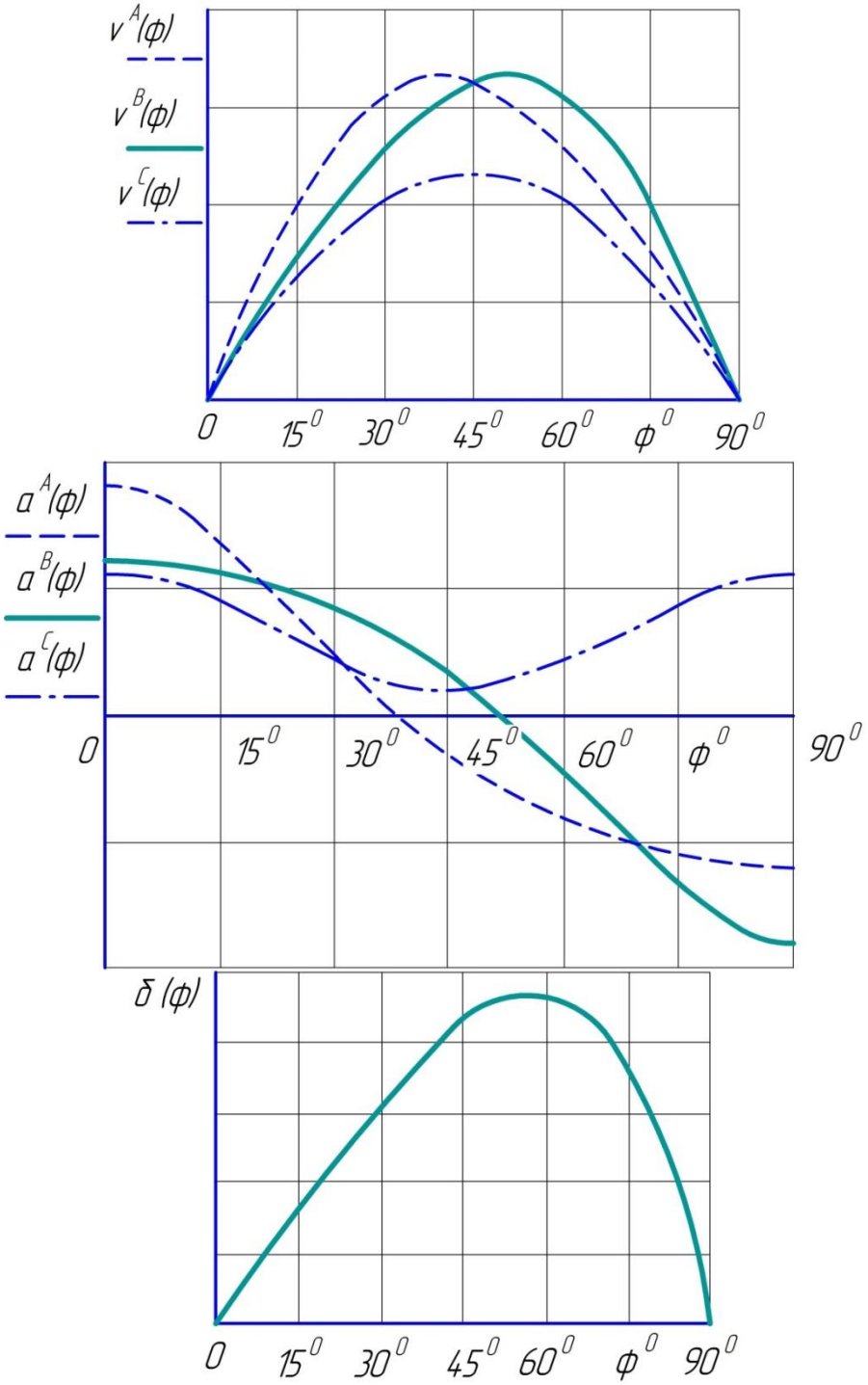

Figure 6. Result of kinematic analysis

Conclusions

This article describes the design of the Fairchild mechanism, carries out its structural and kinematic analysis, and kinematic parameters are obtained by the analytical method. Using two approaches, expressions were obtained that describe the theoretical and true profiles with cams. Despite certain disadvantages of the mechanism (the abundance of moving parts, the presence of high gears), it combines the advantages of the coupling and mechanisms with cams for piston machines.

References

1. Bugayets E. His Majesty - Efficiency // Engine. - 2003. - No. 1,2,3,4,5,6. - 2004. - No. 1,2,3.
2. Balandin S.S. Rodless piston internal combustion engines - M: Mechanical Engineering, 1968. - 152 p.
3. Frolov V.K. Rotary air motor. Patents SU 1562497 (A1 51 (5) F02 B 57/00), SU 1679038 A1 (51 (5) F01 B 1/01).
4. Artobolevsky I.I. Theory of mechanisms and machines. - M .: Nauka, 1988 .-- 640 p.
5. Turakhonov A.S. Technology of metals. - The Teacher Publishing House, 1974. - 398 p.